Pure Appl. Chem., Vol. 81, No. 8, pp. 1385–1396, 2009.
doi:10.1351/PAC-CON-08-08-35

Layered silicate films with photochemically active porphyrin cations*

Alexander Čeklovský[1,‡], Adriana Czímerová[1], Kamil Lang[2], and Juraj Bujdák[1]

[1]Institute of Inorganic Chemistry, Slovak Academy of Sciences, Dúbravská cesta 9, 845 36 Bratislava, Slovakia; [2]Institute of Inorganic Chemistry, v.v.i., Academy of Sciences of the Czech Republic, 250 68 Řež, Czech Republic

Abstract: The objective of this study was to prepare and characterize hybrid films based on layered silicates with a tetracationic porphyrin dye 5,10,15,20-tetrakis(*N*-methylpyridinium-4-yl)porphyrin (TMPyP) intercalated in the inorganic matrix. The properties of the TMPyP cations in the materials were compared with those of other systems (solutions, colloids) characterized mainly by absorption and fluorescence spectroscopies. Linearly polarized absorption spectroscopy, X-ray diffraction (XRD), and fluorescence microscopy were used as well. Using appropriate layered silicate templates, applying the premodification of the inorganic component with hydrophobic alkylammonium surfactants, and selecting an appropriate method, one can prepare the materials of broadly variable spectral properties of the dye. The spectral variation takes place while preserving the photochemical activity of TMPyP. The interpretations of spectral changes are based on the structural changes of the TMPyP molecules adsorbed on layered silicate surface related to the flattening of cationic pyridinium substituents.

Keywords: clay minerals; layer charge; smectites; porphyrin; fluorescence spectroscopy; visible spectroscopy; intercalation.

INTRODUCTION

Interactions between layered inorganic compounds as the host matrices and organic molecular chromophores have been the subject of numerous studies [1–8]. The photofunctional properties of dye supramolecular systems in solutions are significantly different from those of solid-state hybrid materials [9]. Variable compositions and structures achievable via applying dyes of different types, various inorganic hosts, and other components lead to the materials of desired photophysical and -chemical properties, potentially applicable in various industrial fields such as tunable solid-state lasers [10], optical devices, memory storage media, etc. [11].

Clay minerals and related synthetic materials represent an important group of solid layered materials. Basically, clay minerals are hydrous aluminosilicates composed of fine particles [12,13]. They are able to swell in aqueous solutions leading to the formation of colloidal dispersions, suspensions, or gels with a dispersed phase built from the microscopic colloid particles of a diameter smaller than 2 μm having the thickness of several nm [14,15]. The most interesting properties typical for smectites, the

*Paper based on a presentation at the 8th Conference on Solid State Chemistry, 6–11 July 2008, Bratislava, Slovakia. Other presentations are published in this issue, pp. 1345–1534.

‡Corresponding author: Permanent address: Institute of Inorganic Chemistry, Slovak Academy of Sciences, Bratislava, SK-845 36, Slovak Republic; Tel.: 00421-2-59410 433; E-mail: alexander.ceklovsky@gmail.com

subgroup of clay minerals, include swelling, ion-exchange properties, the formation of stable colloidal dispersions, large surface area accessible for the adsorption of various compounds, and the ability to intercalate organic molecules.

Dye molecules have a tendency to form molecular aggregates upon sorption on clay minerals. The charge density of layered silicates controls the molecular aggregation of the dyes of various structural types [16,17]. The aggregation is a crucial problem for the preparation of luminescent hybrid materials based on organic dyes embedded in inorganic solid hosts [18]. The molecular aggregation was assumed to be absent or minimized in the systems based on the dyes of suitable molecular structures, such as ionic porphyrins, e.g., 5,10,15,20-tetrakis(*N*-methylpyridinium-4-yl)porphyrin (TMPyP). Nevertheless, in our previous work [19] studying the hybrid materials based on TMPyP/layered silicate films, we observed significant fluorescent quenching of TMPyP that was interpreted by the formation of sandwich-type porphyrin dimers. In order to improve the photochemical properties of TMPyP we present the hybrid films prepared by the premodification of the inorganic hosts with organic surfactants of variable hydrophobicity and molecular size. The presence of the surfactant modifiers as the third component, as well as the lowering of the concentration of TMPyP, may prevent molecular aggregation and significantly improve the photochemical properties of TMPyP. Taking into account all the above-mentioned factors, our primary objective is to prepare variable hybrid silicate/TMPyP films, to characterize their spectral properties, and to achieve a sufficient photochemical activity of the materials by minimizing the molecular aggregation. The second objective is to control the spectral properties (the energy of light absorption and emission) of the materials.

EXPERIMENTAL

Materials

Fluorohectorite (FHT), Na^+-saturated montmorillonite Kunipia F (KF), and Na^+-saturated hectorite Laponite RD (LAP) were used as representative layered silicates of high, medium, and low layer charge densities, respectively. Synthetic trioctahedral silicates FHT and LAP were obtained from Corning Inc. (USA) and Laporte Industries Co. (UK), respectively. Dioctahedral KF was purchased from Kunimine Industries Co. (Japan). The cation exchange capacity (CEC) values represent the amount of cations that compensate the negative layer charge and are listed in Table 1. The tetra-*p*-tosylate salts of TMPyP (Fig. 1) and 5,10,15,20-tetrakis(*N*-methylpyridinium-2-yl)porphyrin (*o*-TMPyP) were obtained from Frontier Scientific Europe, Ltd. (UK) and Porphyrin Systems (Germany), respectively, and were used as received. For the premodification of layered silicates, the series of alkylammonium salts with various chain lengths was used: dodecyltrimethylammonium chloride (denoted as C12), hexadecyltrimethylammonium bromide (C16), octadecyltrimethylammonium bromide (C18), and dimethyldioctadecylammonium bromide (2C18). The cationic surfactants were obtained from Fluka (purity ≥97 %) and were used as received. Quartz slides (1 × 1") were obtained from SPI Supplies, PA, USA. The slides were transparent in the UV–vis region.

Table 1 CEC values of used layered silicates.

Sample	CEC (mmol/g)
FHT	1.48
KF	1.24
LAP	0.78

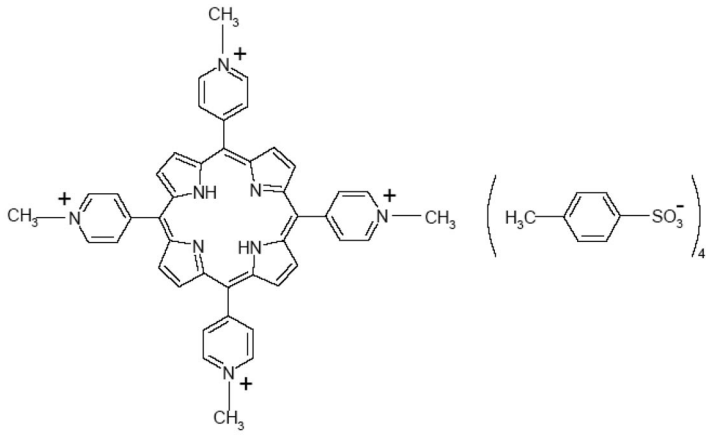

Fig. 1 Structural formula of TMPyP, tetra-*p*-tosylate salt.

Methods

Quartz slides were treated using Piranha solution, 7:3 (v/v) mixture of concentrated H_2SO_4 and 35 % H_2O_2 for 30 min at 90 °C in order to turn the silica surface into hydrophilic and to remove all organic residues and impurities. Aqueous colloidal suspensions of layered silicates (1 g/100 ml) were prepared by mixing the components followed by ultrasonic disaggregation treatment for 30 min. The oriented thin films of layered silicates with TMPyP and *o*-TMPyP on quartz slides were prepared using the following two methods:

(i) Spin-coating of aqueous colloidal suspensions. The samples were injected to fully cover the surface of slides and spin-coated at 1000 rpm/30 s. After drying at 25 °C, the films were immersed into the excess of alkylammonium ions ($c = 10^{-3}$ mol dm^{-3}) and let to achieve the equilibrium for 6 h at 25 °C. In order to remove excess and weakly bound surfactant cations, the films were repeatedly washed with ethanol and dried overnight at 25 °C. Then the films were immersed into the solution of TMPyP ($c = 10^{-4}$ mol dm^{-3}) for 6 h. Prepared films were washed with deionized water and dried at 25 °C. As reference specimens, the films without surfactant premodification were prepared. The films prepared by spin-coating are denoted by suffix "SC". For example, TMPyP/FHT_{SC} relates to the film prepared by spin-coating of FHT followed by the intercalation of TMPyP. The same film premodified with C12 is denoted by TMPyP/C12/FHT_{SC}.

(ii) Casting layered silicate/TMPyP mixtures. The aqueous colloidal dispersions of the silicates (0.5 g/100 ml) were mixed with the solution of TMPyP ($c = 10^{-3}$ mol dm^{-3}) to reach the final TMPyP concentration of 10^{-4} mol dm^{-3}. The loading of TMPyP was 0.08 mmol/g, which is in the scale of a few per cent of the CEC values of the silicates. It prevents molecular aggregation of TMPyP. The mixtures were directly cast on quartz slides and dried at 25 °C. The names of the films are marked with the suffix "CAST". For example, the film prepared by casting of the TMPyP/FHT colloidal dispersion is denoted by TMPyP/FHT_{CAST}.

The aqueous solutions of TMPyP (10^{-4} mol dm^{-3}) and corresponding colloidal dispersions with the silicates (0.08 mmol/g) were prepared as the reference materials. The solutions, colloidal dispersions, and the films of *o*-TMPyP were prepared under the same conditions as those with TMPyP.

X-ray diffraction (XRD) patterns were recorded on a diffractometer Bruker D8 Discover (Cu-K radiation, 40 kV/30 mA). The UV–vis absorption spectra were recorded in the region 350–700 nm by a Cary 100 UV–vis spectrophotometer (Varian). Linearly polarized UV–vis spectra were performed using a Glan-Taylor polarizer (PGT-S1G). Series of the spectra were recorded using both the *x*- and *y*-polarized light, varying the angle between the surface normal of the film specimen and the direction

of the light propagation at 0°, +70°. Absorption intensities were corrected for the substrate and the host material absorptions to obtain absorption intensity of porphyrin chromophores only. The fluorescence spectra were measured on a Perkin–Elmer LS 50B luminescence spectrophotometer. All fluorescence emission spectra were corrected for the characteristics of the detection monochromator and photomultiplier using the fluorescence standards.

Confocal fluorescence and fluorescence lifetime imaging microscopy (FLIM) were carried out on an inverted epifluorescence confocal microscope MicroTime 200 (PicoQuant, Germany). We used a configuration containing a pulsed diode laser (LDH-P-C-440, 440 nm, PicoQuant) providing 80 ps pulses at 40 MHz repetition rate, dichroic mirror 505DRLP, interference filter transmitting 650–730 nm, water immersion objective (1.2 NA, 60×) (Olympus), and detector PDM SPAD (MPD, USA). A module Picoharp 300 (PicoQuant, Germany) recorded the photon events in a time-tagged time-resolved (TTTR) mode enabling the reconstruction of the lifetime histogram for each pixel. In order to minimize the pile-up effects, a low power of 1.5 μW at the back aperture of the objective was chosen.

RESULTS AND DISCUSSION

UV–vis absorption spectra

Films

Figure 2 shows representative absorption spectra of TMPyP in aqueous solution, colloidal dispersion with KF, and representative films. Typically, free-base TMPyP absorption spectrum shows two electronic transitions in the visible region: a Soret band at 421 nm and four Q-bands in the range 514–640 nm. The spectra of TMPyP/KF systems are systematically red-shifted. The extent of the shift depends on the type of TMPyP/KF hybrid system. The shift increases in the following order: aqueous colloidal dispersion, the spin-coated film, the film prepared by casting the dispersion. The $TMPyP/KF_{CAST}$ film is characterized by the Soret absorption maximum at the significantly lower energy (487 nm). The shift with respect to the solution is equal to an energy difference of about 3200 cm^{-1}. In the case of solid films, the Soret bands that are broadened may reflect the distribution of the TMPyP molecules in a heterogeneous chemical environment. The Q-band region is also significantly changed. The spectral changes can be assigned either to the formation of molecular aggregates or structural changes of the chromophore. The protonation of porphyrin pyrrole nitrogen atoms can be

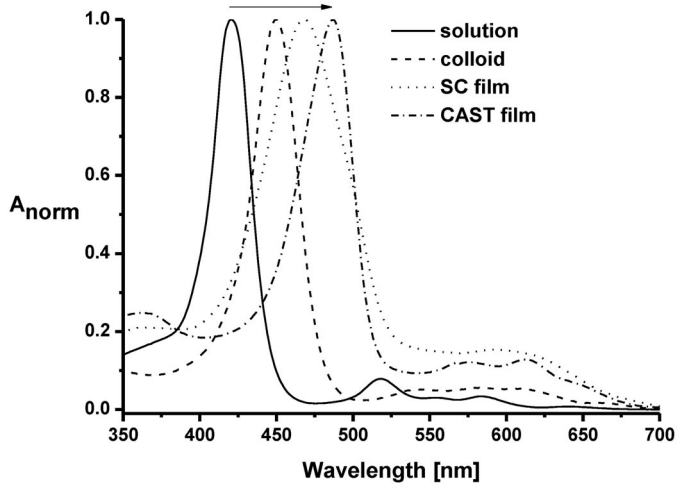

Fig. 2 Absorption spectra of TMPyP/KF systems. Spectra are normalized.

excluded due to the non-acidic nature of the clay hosts. The molecular aggregation of TMPyP in films can be excluded because of a very low loading.

The most plausible explanation of the spectral variations is based on the structural changes of the porphyrin molecules. The trends of the Soret band shifts (Fig. 2) can be explained by the flattening of the TMPyP molecules in dependence on properties of the chemical environment. The flattening of the TMPyP molecules occurs via the changes of the dihedral angle between the pyridinium substituents and the porphyrin moiety from a nearly parallel to an essentially coplanar orientation [20–22]. The driving force of the flattening in the colloids is electrostatic attraction between dye cations and the surface of colloidal particles. The flattening enables electrostatic association between the surface and TMPyP cations via decreasing the distance between positively charged nitrogen atoms of the pyridinium substituents and negatively charged oxygen atoms of the siloxane layer. This effect can be even more significant in solid films because TMPyP cations are intercalated between two adjacent silicate layers. Therefore, the Soret absorption bands are more shifted. The TMPyP/KF_{SC} film is likely composed of monomolecular layers of flatly arranged dye cations between the silicate layers. The XRD patterns (not shown) confirm this structural model with an interlayer distance of 0.59 nm (d_{001} = 1.55 nm), which approximately equals the thickness of the TMPyP cation. Based on the shift of the Soret band (470 nm), the flattening in this film appears to be more significant than in the dispersion. The largest shift of the Soret band observed for the TMPyP/FHT_{SC} films can also be interpreted in terms of the flattening of the TMPyP molecules. The amount of porphyrin in the film with respect to that of the inorganic component is much lower. Only a minor part of the silicate surface is covered by the porphyrin molecules; the majority of exchangeable Na^+ cations remains unchanged. The basal spacing d_{001} (1.27 nm) determined from the XRD patterns (not shown) indicates an interlayer distance of about 0.3 nm. This value is typical for dry Na^+-saturated montmorillonite, reflecting the presence of Na^+ cations with monomolecular layers of water. The sites with TMPyP cations, which would be characterized with significantly larger spacing, were not observed. The low interlayer expansion in Na^+-saturated montmorillonite (KF) further contributes to the flattening of the TMPyP molecules. If TMPyP ions did not change their structure to a more flat conformation, two sites of more and less expanded interlayers representing TMPyP and hydrated Na^+ ions would have to coexist, which might not be favorable from the viewpoint of the energy of the system.

The similar shifts of the Soret bands (464 and 486 nm) with respect to the solution were also observed for the LAP films (not shown). The interlayer distance could not be determined by XRD because of a low signal due to a lack of large LAP scattering domains, which is related to the small size of LAP particles.

An interesting spectral feature is observed in the FHT films. The comparison of the TMPyP/FHT_{SC} and TMPyP/FHT_{CAST} films is shown in Fig. 3. The spectrum of the TMPyP/FHT_{CAST} film indicates the presence of more than one spectral form of TMPyP characterized by two well-resolved Soret bands absorbing at 434 and 475 nm. The TMPyP/FHT_{SC} film has the absorption band only at a lower wavelength of 440 nm. The presence of two porphyrin forms in the TMPyP/FHT_{CAST} film is specific to this silicate. This anomaly could be explained by the properties of FHT, such as a high layer charge and low expandability [23]. The low expandability of FHT might contribute to a more heterogeneous distribution of adsorbed TMPyP cations. The FHT colloidal suspension used for the casting of the films is not probably composed of single FHT layer particles but rather of crystallites and layer aggregates. This could cause a larger local concentration of TMPyP cations at the fraction of accessible surface, which might lead to the formation of molecular assemblies. The high layer charge of FHT (see CEC value in Table 1) could also induce the formation of the assemblies. Due to the high charge density, negatively charged sites are not efficiently saturated by adsorbed individual TMPyP cations inducing dimerization necessary for the balancing of the total charge. Using linearly polarized spectroscopy, we compared the orientation angles of the transition dipole moments of TMPyP cations. Applying *X*-polarized light at a film tilting angle 70º (Fig. 4), the absorption of the band at the lower wavelengths less decreases than that at the longer wavelengths. The molecules represented by the band

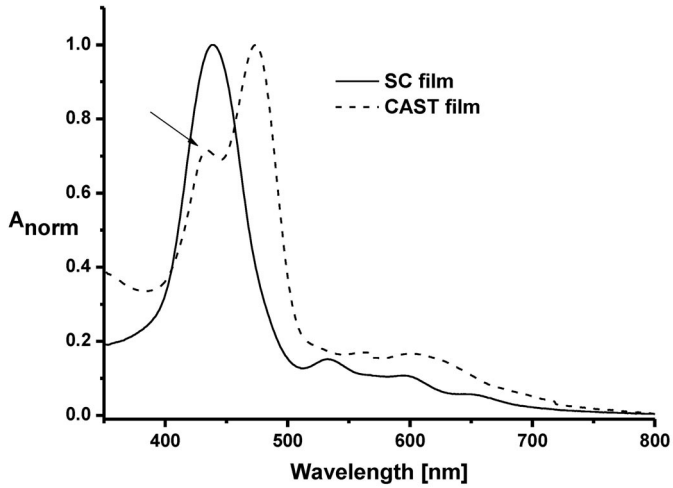

Fig. 3 Absorption spectra of the TMPyP/FHT$_{SC}$ and TMPyP/FHT$_{CAST}$ films. Spectra are normalized.

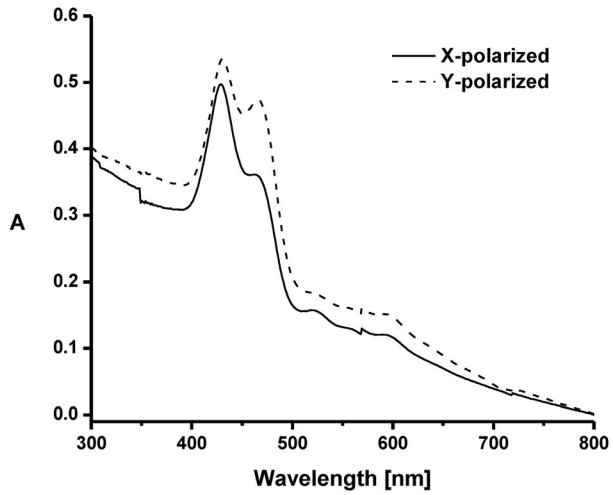

Fig. 4 Linearly polarized absorption spectra of the TMPyP/FHT$_{CAST}$ film at a film tilting angle 70°.

at the longer wavelengths are more planar with respect to the silicate layers than those at the lower wavelengths. Although the difference is rather small, the larger inclination of the porphyrin ring can indicate a partial dimerization between TMPyP cations.

In order to verify the molecular flattening effects, solution, colloidal dispersions and films were prepared using tetracationic porphyrin 5,10,15,20-tetrakis(*N*-methylpyridinium-2-yl)porphyrin isomeric to TMPyP with *N*-methyl substituents in the ortho position (*o*-TMPyP). The methyl substituents sterically prevent or minimize the rotation of the pyridinium rings, i.e., minimize the flattening of the molecule. Evidently, in the case of *o*-TMPyP, the electrostatic interactions between cationic substituents and silicate surface are favored with tilted pyridinium rings. The flattening of *o*-TMPyP is not favorable, and for the dispersions and the films much lower spectral changes can be expected. Indeed, much lower shifts of the Soret and Q-bands were observed independently on the silicate template. The Soret band of *o*-TMPyP aqueous solutions is slightly shifted from 413 to 421 nm in the KF montmorillonite dispersions. The Soret bands are shifted to 425 and 428 nm for the *o*-TMPyP/KF$_{SC}$ and

o-TMPyP/KF_{CAST} films, respectively. The largest shift presents the energy decrease of ~850 cm^{-1}, which is almost four times less than that observed for TMPyP. Similar changes were observed for the films based on *o*-TMPyP and FHT and LAP reaching the positions of the Soret bands at 423 and 428 nm, respectively.

Films premodified with alkylammonium cations

Figures 5a and 5b show the TMPyP absorption spectra in the films based on FHT and LAP pre-intercalated with alkylammonium cations. The cations were used as inert and photochemically inactive molecular spacers to regulate the TMPyP intercalation. The premodification can be important in preventing the molecular aggregation of the chromophores, thus preserving their photochemical activities [9,19]. The absorbances of the Soret bands continually decrease as the size of alkylammonium surfactant cations increase. The trend can be explained by the fact that larger alkylammonium cations cover a major part of the silicate surface or occupy the interlayer space. Then a little space is available for the intercalation of TMPyP cations. The positions of the Soret bands are not significantly changed in the FHT or LAP series. The Soret bands of the FHT films are at shorter wavelengths (440 nm) than those of the LAP films (465 nm) (Fig. 5), which could indicate differences in the conformation of the TMPyP moiety. TMPyP cations in the alkylammonium-modified LAP films probably have a flatter molecular conformation than those in the films based on FHT. This feature may be related to the layer charge density. The high layer charge of FHT causes the accumulation of the cationic surfactants in large quantities, leading to large basal spacing. For example, FHT modified with C18 cation is characterized by heterogeneous alkylammonium arrangement with a main basal reflection of d_{001} = 4.2 nm determined by XRD (not shown). The large d_{001} value is assigned to perpendicularly oriented alkylammonium cations in the interlayer space. The surface of FHT is densely occupied by cationic head-groups of the surfactant molecules due to the large charge density keeping the hydrophobic phase in the middle of the interlayer space. There is a little space for TMPyP cations adsorbed in the second step, unless a part of

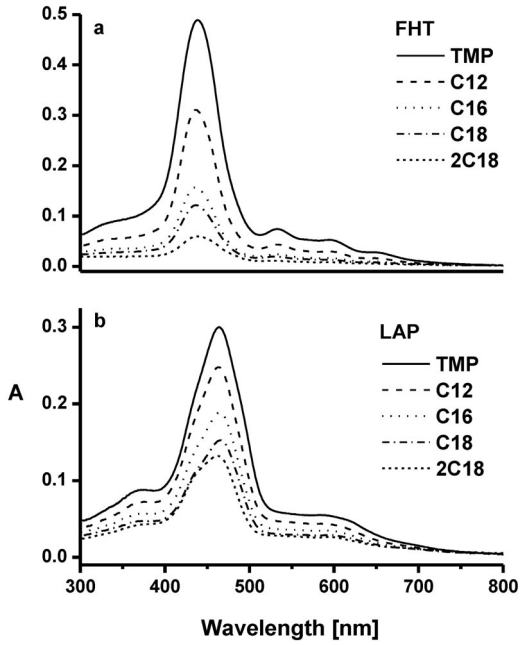

Fig. 5 Absorption spectra of the TMPyP/FHT (a) and TMPyP/KF (b) films premodified with alkylammonium cations.

the surfactant is replaced. Indeed, the adsorption of TMPyP on the FHT/C18 film leads to the reduction of a basal spacing to 3.9 nm, which can be assigned to a partial replacement of surfactant cations during TMPyP adsorption. Thus, the mechanism of TMPyP intercalation in the FHT film is analogous to the dissolution of TMPyP in the hydrophobic phase of the surfactant molecules. LAP is an antipode to FHT concerning the layer charge density. The cationic groups of the surfactants are less dense and likely provide a sufficient surface for the adsorption of TMPyP cations. In this case, the direct interaction of secondarily adsorbed TMPyP cations with the silicate basal surface is more probable. The association could induce a more significant flattening of the TMPyP moiety as reflected by a larger red shift of the Soret bands.

Fluorescence spectroscopy

Figure 6 depicts the steady-state emission spectra of TMPyP aqueous solution, TMPyP/KF aqueous colloidal dispersion, and TMPyP/KF_{CAST}. Similar to the absorption spectra, there are red shifts of the emission bands of the hybrid systems. The spectra are composed of two bands with the maxima at 690 and 755 nm, and 715 and 790 nm. If the energies of the transitions of the dispersion and the film are compared, the shifts of both bands are similar (~520 cm^{-1}). The shifts of the absorption and emission bands to longer wavelengths are not likely related to the formation of dye molecular aggregates although a red shift of the absorption bands (Fig. 2) could indicate the formation of J-type assemblies [9,21]. The systematic decrease of the energies of absorbed and emitted light indicates the structural changes of the TMPyP molecules as discussed above. The spectra indicate the presence of one dominant species in TMPyP/KF. If any other species is present, it is not discerned by absorption or fluorescence spectroscopies.

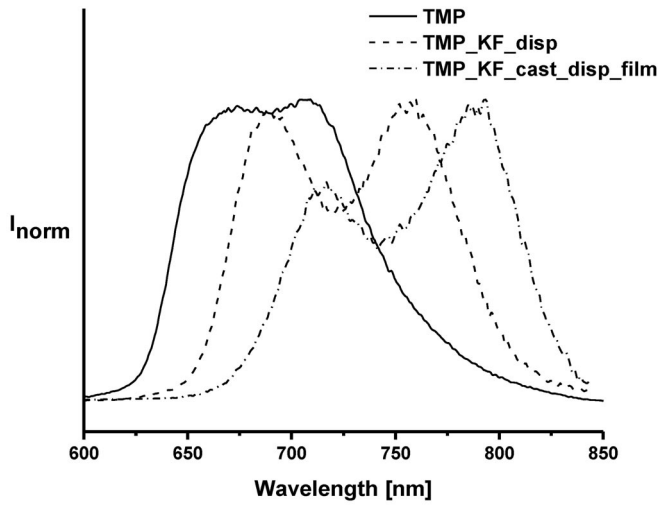

Fig. 6 Fluorescence spectra of TMPyP solution (solid line), TMPyP/KF water dispersion (dashed line), and the TMPyP/KF_{CAST} film (dash-dotted line). Spectra are normalized.

On the other hand, two Soret bands were recognized in the TMPyP/FHT_{CAST} films (Fig. 3). The emission spectra significantly depend on the excitation wavelength in the Soret band region (Fig. 7b). The excitation at 430 nm leads to the emission characterized by the band at 720 nm with two broad shoulders at shorter (~660 nm) and longer wavelengths (~780 nm). The excitation at 475 nm leads to a marked change in the emission spectrum. The shoulder nearby 660 nm disappears in favor of two equally intensive emissions at 720 and 780 nm. The excitation spectra were measured to identify the absorption spectra of fluorescent active species in the film (Fig. 7a). The emission at 660 nm is associated with the species having the absorption band at 434 nm. This spectrum is similar to the absorption

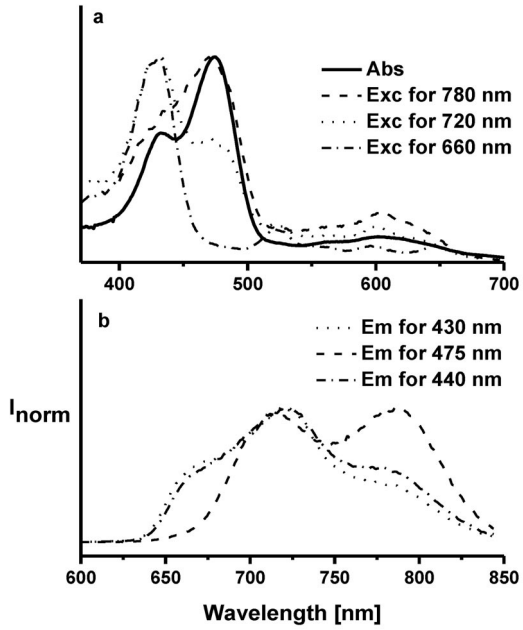

Fig. 7 Spectra of the TMPyP/FHT$_{CAST}$ film. (a) Absorption (Abs) and excitation (Exc) spectra. (b) Emission spectra (Em).

spectrum of the TMPyP/FHT$_{SC}$ film (Fig. 3). Hence, the film prepared by the casting of the FHT/TMPyP dispersion contains two TMPyP species; one of them is present in the film prepared by the dye intercalation (TMPyP/FHT$_{SC}$). The emission at 780 nm (Fig. 7b) is associated with the component absorbing at longer wavelengths. The excitation spectrum recorded at 780 nm indicates significantly different electronic properties of the second species: both the position of the Soret band and the spectral shape in the Q-band region are different.

The films prepared by the intercalation of TMPyP into organically premodified samples exhibit different fluorescence properties. The fluorescence emission appears to be dependent on inorganic template properties and not on the size of the surfactant. Figures 8a and 8b show the representative spectra of the films prepared by the TMPyP intercalation into the FHT and LAP films premodified with C12 and 2C18. The films based on LAP exhibit only a slight variation with the size of the surfactant used for the modification. The spectrum of the TMPyP/C12/LAP$_{SC}$ film has an approximately equally intensive doublet. The TMPyP/2C18/LAP$_{SC}$ film with the largest size surfactant 2C18 has the first emission band partially shifted to shorter wavelength while the emission intensity of the second band is lower. A similar trend is observed in the absorption spectra of these films (Fig. 5). The films modified with the same surfactants but based on FHT exhibit different properties. The emission spectra are not resolved and have only one broad peak envelope at 700–715 nm with a tailing at longer wavelengths. A slight shift to lower wavelengths, when the size of the surfactant increases, is observed as well.

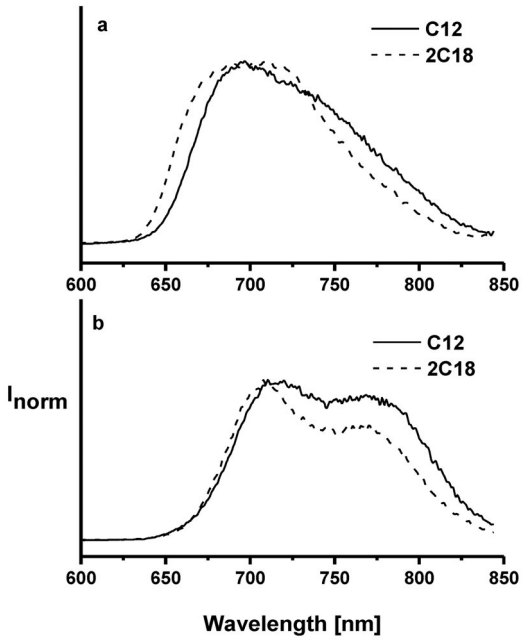

Fig. 8 Emission spectra of the TMPyP/FHT$_{SC}$ (a) and TMPyP/LAP$_{SC}$ films (b) premodified with C12 and 2C18 cations. Spectra are normalized. Excitation wavelength was 440 nm with exception of the TMPyP/2C18/LAP$_{SC}$ film (460 nm).

Confocal fluorescence and fluorescence lifetime imaging microscopy

After determining the integral fluorescence properties, we apply confocal fluorescence microscopy to specify the fluorescence intensity (Figs. 9a,b) and lifetime distributions in the bulk of the hybrid films. The intensity images indicate that LAP and KF films are mostly homogeneous with some small regions of larger intensity that can be explained through the presence of more concentrated areas of fluorescent porphyrin. The homogeneous distribution of TMPyP in LAP is evidenced by the homogeneous intensity image with no indications of porphyrin aggregation within the microscope resolution (lateral ~250 nm) (Fig. 9a). The fluorescence emission decays with at least two lifetimes of 0.9 and 2.3 ns, and their homogeneous spatial distributions are not affected by the presence of the surfactants while the values slightly increase to 1.2 and 3.5 ns in the TMPyP/C38/LAP$_{SC}$ film. The lifetime values are comparable with those of 0.7, 3.2, and 3.8 ns recorded for TMPyP in synthetic clay Sumecton SA [6]. The TMPyP/LAP$_{CAST}$ is more heterogeneous as documented by the intensity image (Fig. 9b). The fluorescence decays are characterized by two fluorescence lifetimes of 1.2 and 4.3 ns. The KF films also appear relatively homogeneous with two fluorescence lifetimes of 0.7 and 2.1 ns not affected by C12. These values are similar to those recorded in LAP and might indicate that TMPyP fluorescence reflects a similar environment in both spin-coated films based on LAP and KF. The FHT films are characterized by heterogeneous TMPyP distributions and lifetime components of about 0.9, 2.2, 3.5, and 4.8 ns. The *z*-scans of all hybrid films show that the thickness of the fluorescent spin-coated films slightly varies from 2.1 to 2.4 μm while the cast films are more thick (4–6 μm).

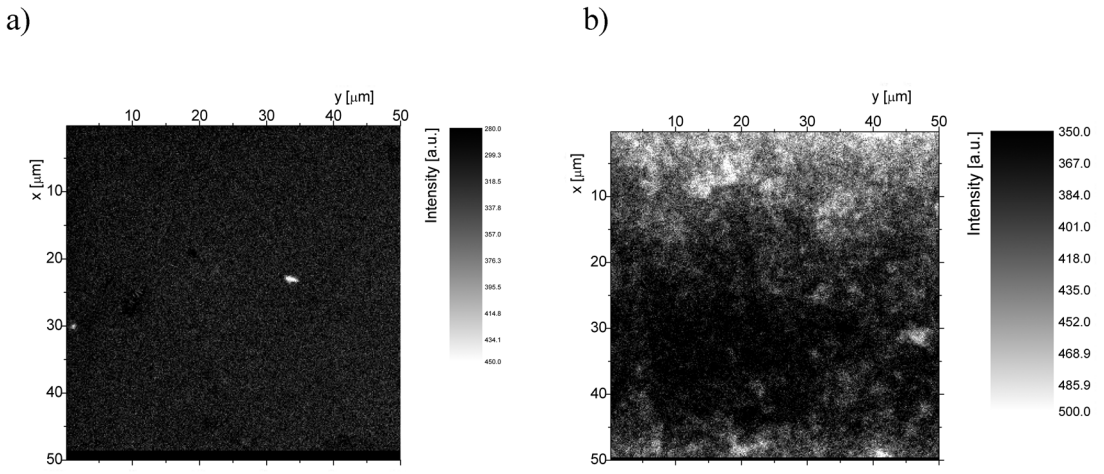

Fig. 9 Fluorescence intensity image of the TMPyP/LAP$_{SC}$ (a) and TMPyP/LAP$_{CAST}$ (b) in the color scale recorded at the surface (50 × 50 μm, *x*–*y* scan, *z* = 0). The film is excited at 440 nm, and fluorescence intensity is recorded within the 650–730 nm region.

ACKNOWLEDGMENTS

This work was supported by the Slovak Research and Development Agency under contract No. APVV-51-027405, the Grant Agency VEGA (2/6180/27), the Czech Science Foundation (No. 203/06/1244, to K. L.), and the Grant Agency of the Academy of Sciences of the Czech Republic (No. KAN 100500651, to K. L.). The authors thank Jan Sýkora and Martin Hof (J. Heyrovský Institute of Physical Chemistry, v.v.i., ASCR, Praha, Czech Republic) for the fluorescence microscopy measurements.

REFERENCES

1. R. Sasai, N. Iyi, T. Fujita, F. López Arbeloa, V. Martínez Martínez, K. Takagi, H. Itoh. *Langmuir* **20**, 4715 (2004).
2. Z. Chernia, D. Gill. *Langmuir* **15**, 1625 (1999).
3. M. Eguchi, S. Takagi, H. Tachibana, H. Inoue. *J. Phys. Chem. Solids* **65**, 403 (2004).
4. J. Bujdák, N. Iyi, Y. Kaneko, A. Czímerová, R. Sasai. *Phys. Chem. Chem. Phys.* **5**, 4680 (2003).
5. P. M. Dias, D. L. A. de Faria, V. R. L. Constantino. *J. Inclusion Phenom. Macrocycl. Chem.* **38**, 251 (2000).
6. S. Takagi, T. Shimada, M. Eguchi, T. Yui, H. Yoshida, D. A. Tryk, H. Inoue. *Langmuir* **18**, 2265 (2002).
7. C. Sanchez, B. Lebeau, F. Chaput, J. P. Boilot. *Adv. Mater.* **15**, 1969(2003).
8. Ch. A. Schalley, A. Lutzen, M. Albrecht. *Chem.—Eur. J.* **10**, 1072 (2004).
9. J. Bujdák. *Appl. Clay Sci.* **34**, 58 (2006).
10. R. Sasai, N. Iyi, T. Fujita, F. L. Arbeloa, V. M. Martinez, K. Takagi, H. Itoh. *Langmuir* **20**, 4715 (2004).
11. C. Sanchez, B. Julián, P. Belleville, M. Popall. *J. Mater. Chem.* **15**, 3559 (2005).
12. B. Číčel, I. Novák, I. Horváth. *Mineralógia a Kryštalochémia Ílov*, VEDA, Vydavatel'stvo SAV, Bratislava (1981).
13. A. C. D. Newman. *Chemistry of Clays and Clay Minerals*, Monograph No. 6, Mineralogical Society, New York (1987).
14. K. G. Theng. *The Chemistry of Clay-Organic Reactions*, Adam Hilger, London (1974).

15. R. E. Grim. *Clay Mineralogy*, International Series in Earth and Planetary Sciences, 2nd ed., Pergamon Press, New York (1968).
16. J. Bujdák, P. Komadel. *J. Phys. Chem. B* **101**, 9065 (1997).
17. J. Bujdák, N. Iyi. *Clays Clay Miner.* **50**, 446 (2002).
18. A. Czímerová, N. Iyi, J. Bujdák. *J. Colloid Interface Sci.* **306**, 316 (2007).
19. A. Čeklovský, A. Czímerová, M. Pentrák, J. Bujdák. *J. Colloid Interface Sci.* **324**, 240 (2008).
20. Z. Ou, H. Yao, K. Kimura. *J. Photochem. Photobiol., A* **189**, 7 (2007).
21. S. Takagi, M. Eguchi, D. A. Tryk, H. Inoue. *J. Photochem. Photobiol., C* **7**, 104 (2006).
22. M. Eguchi, H. Tachibana, S. Takagi, H. Inoue. *Res. Chem. Intermed.* **33**, 191 (2007).
23. J. O. Fossum. *Physica A* **270**, 270 (1999).